Research Paper

==

Integrated application of remote sensing and geoelectrical techniques for wastewater percolation mapping at the northern part of Badr city, Egypt

Abeer El-Kenawy[1], Usama Massoud[2], Mohamed Attwa [1,3] and Mohamed Ibrahim[1]

[1]Zagazig University, Faculty of Science, Zagazig, 44519, Egypt
[2]National Research Institute of Astronomy and Geophysics, NRIAG, 11421 Helwan, Egypt
[3] National Authority for Remote Sensing and Space Sciences

***ABSTRACT* :** Water-logging appearance in new urban areas has become one of the most environmental hazards. The purpose of this research is to understand the wastewater flow paths in desert lands. As a case study, the wastewater leakage problem in the northern part of Badr City, Egypt was investigated by applying remote sensing (RS) and direct current (DC) resistivity techniques. Regarding local geological conditions, the relation between subsurface structures, surface topography, and wastewater leakage appearance was delineated. Modern GIS techniques were used to represent wetlands, streams, drainage networks, elevation, surface ponds, and other features. DC resistivity survey in the form of vertical electrical sounding (VES) was conducted to get an overview of the distribution of subsurface layers and structures (faults) considering the borehole and surface geological data. As a result, the general slopes, subsurface structure, and near-surface layers distribution play an important role in water seepage and water-logging on the ground surface. This study answers the question regarding the correlation between water-logging and surface/subsurface factors that control wastewater flow paths in desert lands. Further studies are needed to establish causal relationships and develop preventative measures.

KEYWORDS: Remote sensing; Direct current resistivity; water-logging

----

I.   INTRODUCTION

Every country seeks to decrease stress of overcrowded population in the capitals by putting roots of urbanization on barren lands. Consequently, Egypt has proceeded to take steps to solve the problem of overcrowded population around the Nile Valley, at the beginning of the last decade, in a variety of ways such as desert lands reclamation policy and the construction of new industrial and residential cities: such as the new administrative capital, new Alamein City and Badr City which consider our study area. However, increasing of urbanization counters various nature and human induced geological hazards such as: sand encroachment, pollution of natural sources like pollution of ground water and pollution of soil due to improper disposal of wastewater [1].To avoid these issues, effective planning is required prior to the establishment of industrial cities and new population concentrations. So, surface and near-surface geological structures, magnitudes and history of seismic events and distribution of surface and near-surface clay and/or shale layers are all elements that should be thoroughly investigated and evaluated.

Wastewater leakage is one of the most complicated environmental issues in desert regions and new urban areas. This includes the influence of wastewater on soil, rock stability and groundwater quality [2]. Although stabilization pond systems provide dependable and low-maintenance treatment at a low cost for industrial and municipal wastes, poor design, operation and maintenance needs can have a harmful environmental impact through gully erosion and geological disaster [3]. Furthermore, wastewater leakage/evaporation near cities has a negative impact on public health and sustainable engineering approaches. To manage and solve the predicted geo-environmental problems connected with wastewater overflow and percolation surrounding wastewater evaporation and stabilization ponds, it is necessary first to understand the surface and/or subsurface elements that influence wastewater leakage and water-logging.

Traditionally, geological and hydrogeological techniques such as soil studies, borehole drilling and water chemical analysis have been used to investigate the environmental consequences of wastewater overflow, particularly in new urban areas [4].These direct procedures, however, give only a limited comprehension and spatial information about wastewater flow pathways in dry environments. Remote sensing (RS) and geophysical

approaches, on the other hand, have been used to be useful diagnostic tools for studying the environmental concerns related to wastewater ponds/treatment since they are cost-effective, non-intrusive and rapid [5], [6]
The current case study, Badr City, is one of Egypt's new communities and developed industrial cities. The industrial wastewater from around 195 leather factories (known as Rubiki Leather City) is improperly disposed of into stabilization pond sets and open evaporation ponds in the North-Eastern section of Badr City (Fig. 1). The efficiency of these ponds is dwindling due to hydraulic overloading and a lack of filtration. Based on field observations, wastewater seepage and water-logging have been observed in numerous locations, posing serious environmental hazards.
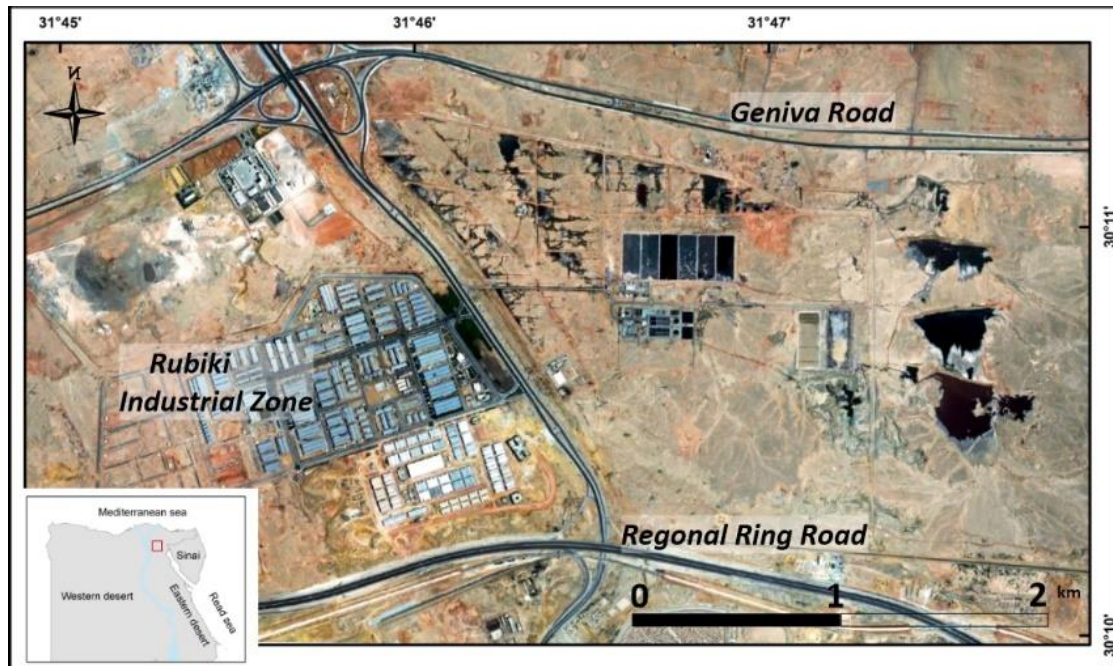

Figure 1: Location map of the study area.

The integration of geographic information system (GIS) technology and remote sensing (RS) data has been developed quickly during the previous few decades. Fortunately, GIS and RS are widely used in ordinary people's everyday lives, where these two exceptional technologies are valuable for location decision making and have been implemented in various types of research scenarios [5], [7].

Indeed, the qualitative and quantitative parameters acquired from RS and GIS data can be used to identify geoenvironmental hazards and mange wastewater. As a result, geological investigations may be combined with multi-GIS data layers to analyze and manage wastewater seepage in arid and semi-arid regions [8]

Geophysical studies are being conducted with the visual inspection of high-resolution RS images and detailed geological analysis. The DC resistivity in particular has been preferred and successfully employed to solve a wide range of technical and geo-environmental challenges [9]. Furthermore, the DC resistivity approach can be employed to connect surface hydrogeological phenomena with subsurface structural elements. So, DC resistivity survey in the form of Vertical Electrical Sounding (VES) was used to show the near surface lithologic heterogeneity and subsurface structure by correlating sounding points results with each other and with the nearest boreholes. From integration between RS and VES data we could precisely detect the factors controlling wastewater seepage paths and water-logging.

The study seeks to provide a systematic method for studying and assessing the existence of waterlogging and wastewater seepage in arid environments. Consequently, a wise plan can be built to reduce similar damage in the future if we understand the elements involved.

II-Local geology.

Our research site was regarded to be a part of the Cairo-Suez district, which is characterized by complicated tectonic setting. According to [10], the structural framework of the Cairo-Suez area is dominated by two primary sets of faults directed E-W and NW, both of which are of the same age. Also, the stratigraphic column of the study area comprises a sequence of Miocene rocks at the base, followed by Pliocene deposits and overlain by Quaternary clastics (Fig. 2).
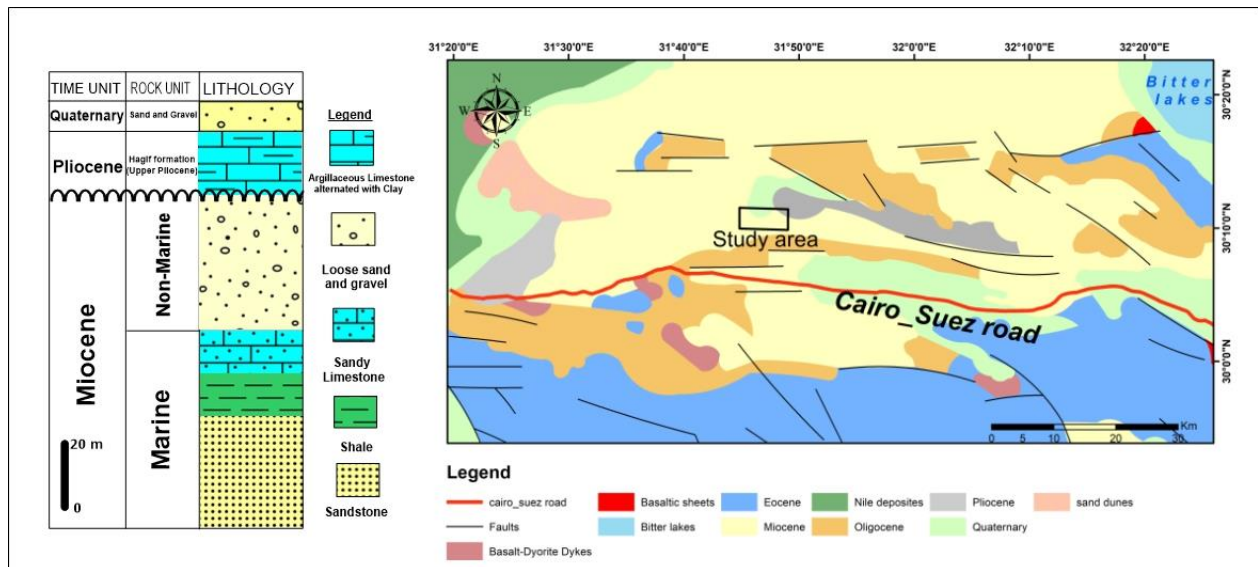
Figure 2: *Structural map of Cairo-Suez district shows the orientation of main faults modified after*[11]*and Composite stratigraphic section of the study area modified after* [12]

According to [13] the Miocene deposits, which come first at the stratigraphic column in the study area, is divided into two units: marine and non-marine unit. The marine Miocene is made up of sandstone, shale and sandy limestone, whereas the non-marine unit is made up of unstratified sand and gravels. The eastern part of the study site, as shown in figure (2), is dominated by Pliocene deposits, which are represented by Hagif Formation. This formation is formed of shallow marine succession (30 m thick) of thick Limestones alternating with shales and shaly sandstone [14]. Quaternary clastics come at the top of succession in the form of sands and gravels.

III-Materials and Methods

Remote Sensing (RS)

The geological and structural settings were collected from real field observations, available map resources, and other sources, in addition to the remote sensing (RS) data given by high-resolution Google Earth (GE) images. A high-quality Digital Elevation Model (DEM) was used to improve the accuracy of topographic variation detection. The various hydrographic characteristics of drainage basins have been widely extracted from available (DEM) via sequential processing steps in various GIS applications. Traditionally, the hydrological modelling tools in ArcGIS are used to construct the flow paths (i.e., drainage networks) that are spatially interconnected all the way through the (DEM) matrix from upstream to outlet each unit cell (i.e., pixel). In general, the processing stages attempt to specify the flow directions of each cell into surrounding ones, and the resulting grid is then used to estimate the arbitrary upstream flow contributing areas for each cell, which is known as flow accumulation [15].Then we can clearly determine the relation between wastewater seepage and topography variation in the study area.

Vertical Electrical Sounding (VES) Method

The VES data were measured at 20 points (Fig. 3) along straight survey lines, as feasible, taking into account our field observations, local geology, surface features and analysis of satellite images. The ground contact resistance was often low because of the presence of wastewater seepage. Because of its higher lateral resolution, Schlumberger array was chosen to gather sounding data for mapping regional subsurface layer distributions and structures throughout the study area. [16].
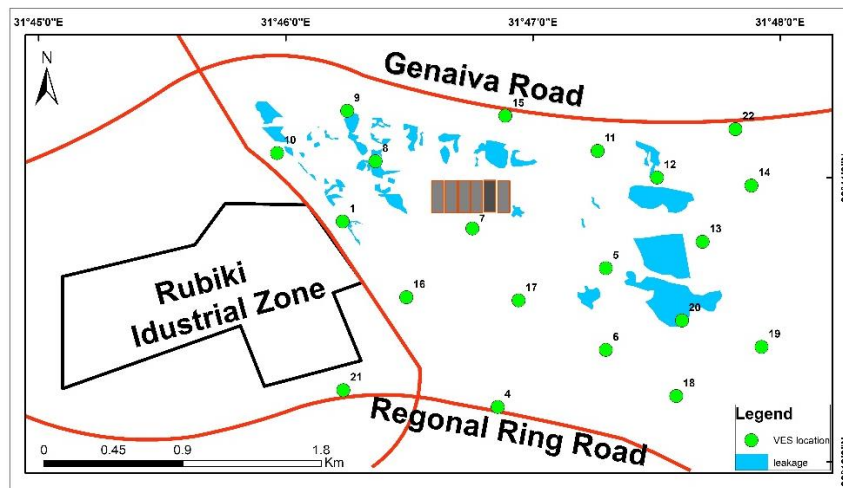
Figure 3: Location map of VES points, oxidation ponds and water-logged soils.

The resistivity data have been acquired in this area using Syscal Pro instrument. The field measurements were carried out by application of the standard Schlumberger electrode configuration with current electrode spacing varying logarithmically from 2 meters to 600 meters. The maximum electrode separation (AB) was 600 meters. The measured (apparent) resistivity values have been analyzed to determine the true geoelectrical parameters (resistivity and thickness) of subsurface layers. The VES data were analyzed by IPI2Win software which is capable of solving electrical resistivity prospecting 1D forward and inverse problem for the commonly used arrays with a big resistivity contrast. The forward problem (Forward Modeling) is solved using the linear filtering. The filters are tested thoroughly and the filtering approach implementation provides fast and accurate direct problem solution for a wide range of models, covering all reasonable geological solutions.

The inverse problem (Inversion) is solved using a variant of Newton`s algorithm of the least number of layers or the regularized fitting minimizing algorithm using Tikhonov`s approach for solving incorrect problems. Priory information on layers, depths and resistivities can be used for regularizing the process of the fitting error minimizing. The inverse problem is solved separately for each sounding curve.

IV-Results and discussion

Remote Sensing

As mentioned before, the main purpose of our research is to understand the main factors that control the wastewater seepage in the new urban areas. The digital elevation model (DEM) was inspected to assess the relationship between geomorphology, topography and paths of wastewater in barren lands. As shown in figure (4), the ground surface elevation of the study area is ranging from 177 to 217m. The highest elevations are concentrated at the southern part of the study area and the elevation decreases towards the north. Also, from DEM we extracted the flow paths (i.e. drainage networks) to determine the main streams in the area of study (Fig. 4).

It can be noticed that the main water-logging appears at lowlands and correspond to the stream directions (i.e. north and north-western trends) which prove that, water seepage is controlled by topography and slopes in the study area. Figure (4) also shows that the wastewater flow pathways are mostly linear. As a result, there is a strong need to better understand the subsurface geological parameters that govern the wastewater flow pathways in such arid area.
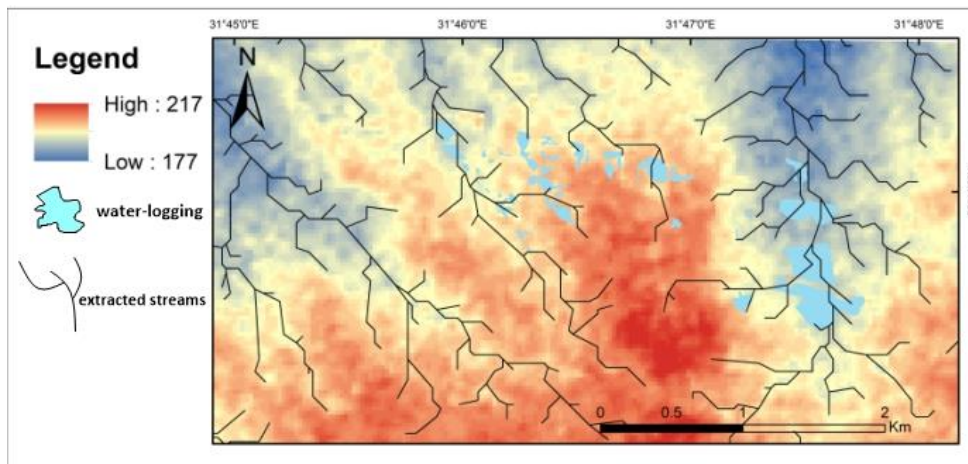
Figure 4: *High resolution digital elevation model (DEM) with extracted streams and location of water-logged.*

VES Results

The interpretation task is the determination of the presence of layers of material of common resistivity. Both curve matching and analytical procedures can be used to identify the presence of resistivity layering (eg. vertical, horizontal, or dipping beds). In this study, the computer program "IPI 2WIN 1-D" was used to calculate the final earth resistivity model, see table 1. The justification of the final model is controlled by calculating the Root-Mean-Square error (RMS-error) between the measured and calculated resistivity values.

The final output of the inversion process is a set of multi-layer models each of them describes the electrical resistivity behavior at its respective location. Selected examples of the 1D models are shown in figures (5, 6, 7 and 8). These models were used to construct 2D stitched cross sections (Fig. 9).
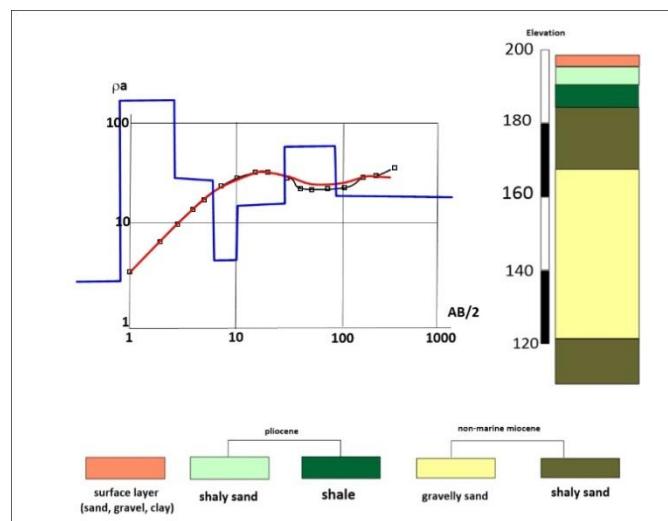

Figure 5: *The inversion results of VES point 9 and its correlated lithologic column.*
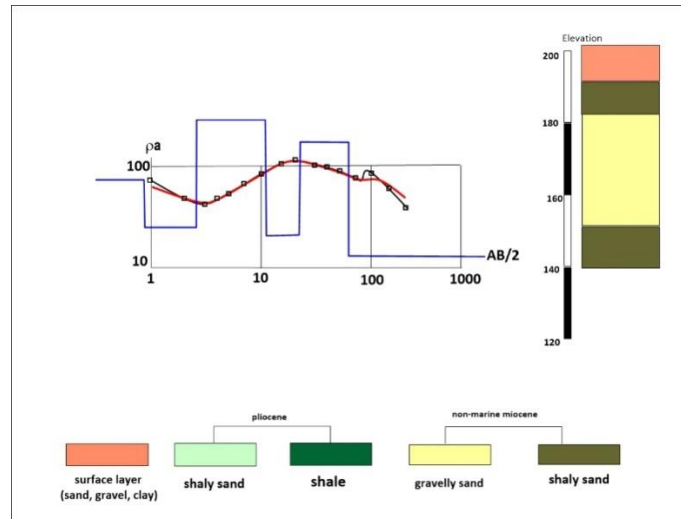
Figure 6: *The inversion results of VES point 7 and its correlated lithologic column.*
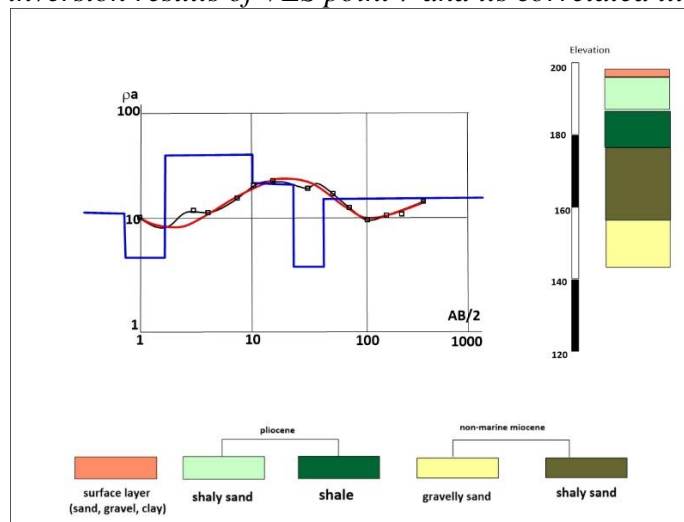

Figure 7: *The inversion results of VES point 5 and its correlated lithologic column.*

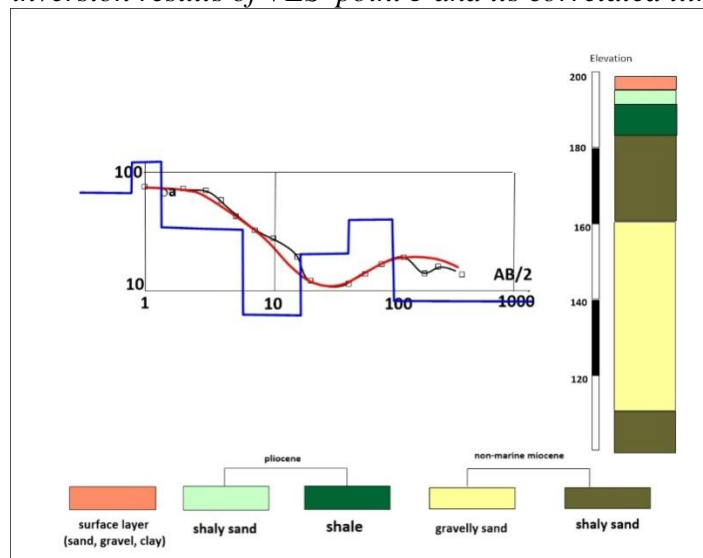***Figure 8:*** *The inversion results of VES point 19 and its correlated lithologic column.*

Figure (9) shows a stitched resistivity section, representative to the study area, travelling between the position of the oxidation ponds and the observed water-logged soils at the research site. Water-logged soils are clearly concentrated on the low to medium resistivity layers (20 Ohm-m), which are correlated with

impermeable to semi-impermeable Pliocene shale and shaly sand, respectively. Furthermore, the borehole information and surface geological data were used to verify the VES data interpretation. The faults map and satellite image lineaments were used to link the inferred structure, i.e., faults, on the produced geoelectrical section which is connected to the observed geoelectrical layers displacement. As a result, water-logging and wastewater flow pathways are connected with the existence of near-surface, low permeability, Pliocene strata and the downthrown side of faults in the southeastern and northwestern regions of the research site.
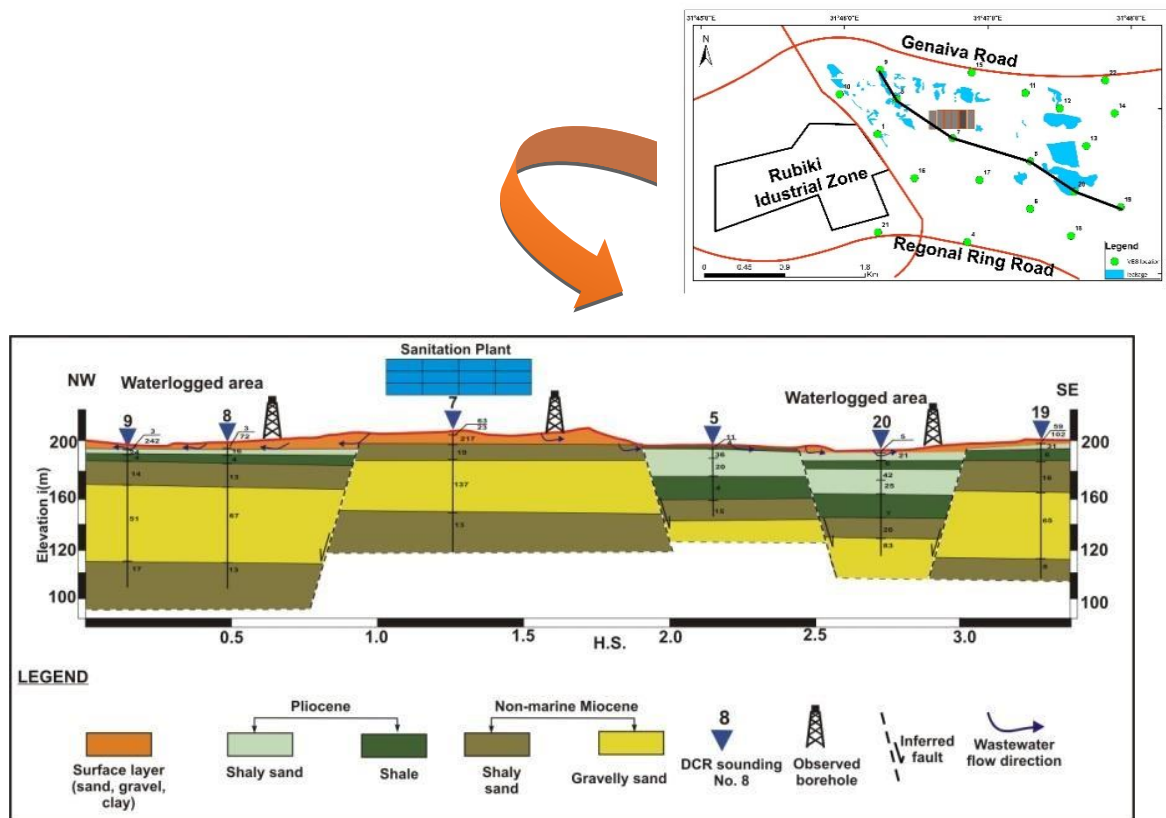

Figure 9: Stitched resistivity section based on VES data inversion results calibrated with surface geological and borehole data showing that the paths of wastewater flow around the oxidation pond are controlled by surface topography, faults, and subsurface layers distribution.

VES No		Layer-1	Layer-2	Layer-3	Layer-4	Layer-5	Layer-6	Layer-7	Layer-8
1	**Resistivity**	30	22.4	11.7	25	5.14	30	3.37	
	Rock name	Surface layer (Sand, Gravel, and Clay).		Pliocene Shaly sand.		Pliocene Shale.	Pliocene Shaly sand.	Pliocene Shale.	
4	**Resistivity**	10.1	80.5	24.8	115	14.5			
	Rock name	Surface layer (Sand, Gravel, and Clay).		Non-Marine Miocene shaly sand.	Non-Marine Miocene Gravelly sand	Non-Marine Miocene shaly sand.			
5	**Resistivity**	11.1	4.44	36.2	20.1	3.7	15		
	Rock name	Surface layer (Sand, Gravel, and Clay).	Pliocene Shale.	Pliocene Shaly sand.		Pliocene Shale.	Non-Marine Miocene shaly sand.		

No.		1	2	3	4	5	6	7	8
6	**Resistivity**	33.1	137	20.6	2.96	22.5			
	Rock name	Surface layer (Sand, Gravel, and Clay).		Pliocene Shaly sand.	Pliocene Shale.	Non-Marine Miocene shaly sand.			
7	**Resistivity**	63.1	22.7	217	19.4	137	12.7		
	Rock name	Surface layer (Sand, Gravel, and Clay).			Non-Marine Miocene shaly sand	Non-Marine Miocene Gravelly sand	Non-Marine Miocene shaly sand		
8	**Resistivity**	3.24	72	16.2	3.73	13.2	66.7	12.9	
	Rock name	Surface layer (Sand, Gravel, and Clay).		Pliocene Shaly sand.	Pliocene Shale.	Non-Marine Miocene shaly sand.	Non-Marine Miocene Gravelly sand	Non-Marine Miocene shaly sand.	
9	**Resistivity**	2.75	242	24.9	4.34	14.4	51.4	17	
	Rock name	Surface layer (Sand, Gravel, and Clay).		Pliocene Shaly sand.	Pliocene Shale.	Non-Marine Miocene shaly sand.	Non-Marine Miocene Gravelly sand	Non-Marine Miocene shaly sand.	
10	**Resistivity**	32	106	34	25	6	13	48	12
	Rock name	Surface layer (Sand, Gravel, and Clay).			Pliocene Shaly sand.	Pliocene Shale.	Non-Marine Miocene shaly sand.	Non-Marine Miocene Gravelly sand	Non-Marine Miocene shaly sand.
11	**Resistivity**	7.46	55	9	5	18	2	18	
	Rock name	Surface layer (Sand, Gravel, and Clay).		Pliocene Shale.		Pliocene Shaly sand.	Pliocene Shale.	Non-Marine Miocene shaly sand.	
12	**Resistivity**	9.4	4.86	84	11	26	9		
	Rock name	Surface layer (Sand, Gravel, and Clay).			Pliocene Shale.	Pliocene Shaly sand.	Pliocene Shale.		
13	**Resistivity**	6.64	1.89	4	14	1	19		
	Rock name	Surface layer (Sand, Gravel, and Clay).		Pliocene Shale.	Pliocene Shaly sand.	Pliocene Shale.	Non-Marine Miocene shaly sand.		
14	**Resistivity**	28	7	1	33	10			
	Rock name	Surface layer (Sand, Gravel, and Clay).	Pliocene Shale.		Pliocene Shaly sand.	Pliocene Shale.			
15	**Resistivity**	331	81.6	18.8	54.4	15			
	Rock name	Surface layer (Sand, Gravel, and Clay).		Non-Marine Miocene shaly sand.	Non-Marine Miocene Gravelly sand	Non-Marine Miocene shaly sand.			
16	**Resistivity**	10.7	17.7	2.48	8.62	76.2	19.5		
	Rock name	Surface layer (Sand, Gravel, and Clay).		Pliocene Shale.		Non-Marine Miocene Gravelly	Non-Marine Miocene shaly sand		
17	**Resistivity**	46.1	30.4	8.84	1.9	13.4	102		
	Rock name	Surface layer (Sand, Gravel, and Clay).		Pliocene Shale.		Non-Marine Miocene shaly sand	Non-Marine Miocene Gravelly sand		
18	**Resistivity**	41	5	16	6	30	162		
	Rock name	Surface layer (Sand, Gravel, and Clay).		Pliocene Shaly sand.	Pliocene Shale.	Non-Marine Miocene shaly sand.	Non-Marine Miocene Gravelly sand		
	Resistivity	58.9	102	30.6	5.83	16.3	64.7	8.33	

19	**Rock name**	Surface layer (Sand, Gravel, and Clay).	Pliocene Shaly sand.	Pliocene Shale.	Non-Marine Miocene shaly sand.	Non-Marine Miocene Gravelly sand	Non-Marine Miocene shaly sand.	
20	**Resistivity**	5.39	21	6	42	25	7	26	83
	Rock name	Surface layer (Sand, Gravel, and Clay).	Pliocene Shaly sand.	Pliocene Shale.	Pliocene Shaly sand.		Pliocene Shale.	Non-Marine Miocene shaly sand.	Non-Marine Miocene Gravelly sand
21	**Resistivity**	813	39.3	5.71	26	78	11.8		
	Rock name	Surface layer (Sand, Gravel, and Clay).			Non-Marine Miocene shaly sand.	Non-Marine Miocene Gravelly sand	Non-Marine Miocene shaly sand.		
22	**Resistivity**	52.6	13.1	100	29	5			
	Rock name	Surface layer (Sand, Gravel, and Clay).			Pliocene Shaly sand.	Pliocene Shale.			

Table 1. summary of Vertical Electrical Sounding results

V CONCLUSION

As a case study, RS and VES data were used to evaluate the occurrence of wastewater leaks in a semi-arid new urban environment. Wadies, streams, drainage systems, elevation, surface ponds and so on were displayed using modern GIS techniques. The DEM-related extracted drainage systems revealed a substantial association between the wastewater flow paths and the main drainage lines over the research site. It meant that the occurrence of surface wastewater leakage is related to general slopes.

In order to analyze land aspects within a RS framework, DC resistivity measurements were taken in the form of VES data to provide us with overview of subsurface layers and structure distribution which play a vital role in controlling wastewater seepage and water-logging on the surface.

The inversion results of the measured VES data revealed that the appearance of wastewater seepage was correlated with near-surface soil heterogeneities and subsurface structures (faults). As a result, wastewater leakage occurs along drainage paths (i.e., lines) that are converged in structural controlled depressions related to faults downthrown. Furthermore, wastewater accumulates above an impermeable near-surface layer, which forms ponds and surface seepage. This impermeable layer is mapped using DC resistivity results as shown in (Fig. 10).

The integration between GIS, RS and geophysical approach provides a helpful strategy to monitor, evaluate and understand the factors that control wastewater seepage and water-logging at desert lands. With this understanding, the bad effects of wastewater in the new urban areas can be mitigated.
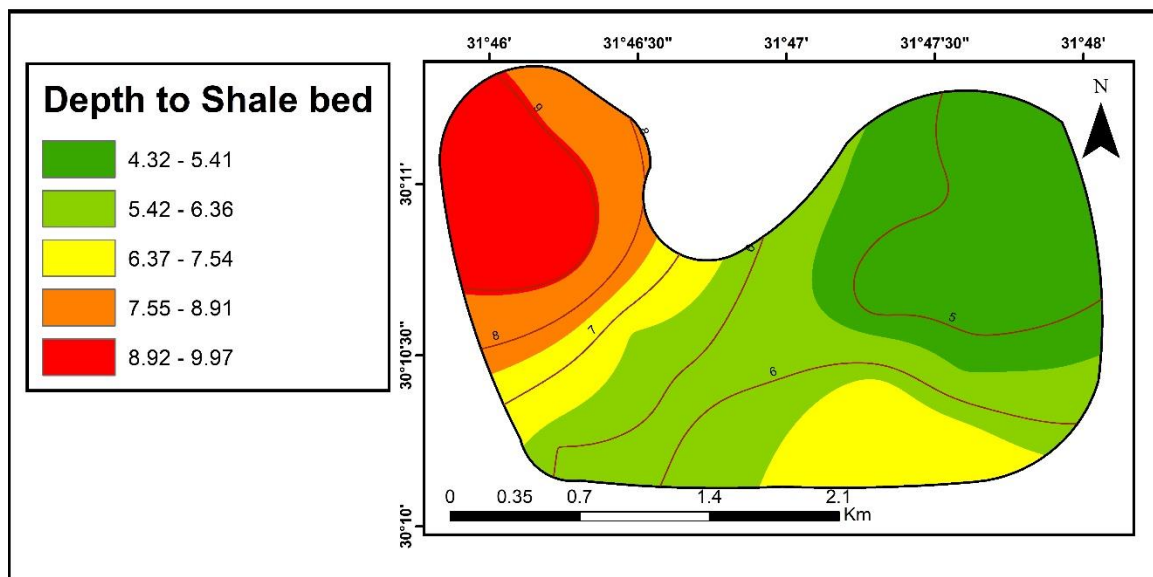
Figure 10: contour map, shows the distribution and depth of shale bed in the study area.

REFERENCES

[1]   A. M. Youssef, Y. A. Zabramwi, F. Gutiérrez, A. M. Bahamil, Z. A. Otaibi, and A. J. Zahrani, "Sinkholes induced by uncontrolled groundwater withdrawal for agriculture in arid Saudi Arabia. Integration of remote-sensing and geophysical (ERT) techniques," *J Arid Environ*, vol. 177, Jun. 2020, doi: 10.1016/j.jaridenv.2020.104132.

[2]   Y. Zhang *et al.*, "A review of preferential water flow in soil science," *undefined*, vol. 98, no. 4, pp. 604–618, 2018, doi: 10.1139/CJSS-2018-0046.

[3]   P. Amoatey *et al.*, "A critical review of environmental and public health impacts from the activities of evaporation ponds," *Science of the Total Environment*, vol. 796. Elsevier B.V., Nov. 20, 2021. doi: 10.1016/j.scitotenv.2021.149065.

[4]   C. Liu *et al.*, "Domestic wastewater infiltration process in desert sandy soil and its irrigation prospect analysis," *Ecotoxicol Environ Saf*, vol. 208, Jan. 2021, doi: 10.1016/j.ecoenv.2020.111419.

[5]   M. Attwa and S. Zamzam, "An integrated approach of GIS and geoelectrical techniques for wastewater leakage investigations: Active constraint balancing and genetic algorithms application," *J Appl Geophy*, vol. 175, p. 103992, 2020, doi: 10.1016/j.jappgeo.2020.103992.

[6]   I. A. El-Magd, M. Attwa, M. el Bastawesy, A. Gad, A. Henaish, and S. Zamzam, "Qualitative and Quantitative Characterization of Municipal Waste in Uncontrolled Dumpsites and Landfills Using Integrated Remote Sensing, Geological and Geophysical Data: A Case Study," *undefined*, vol. 14, no. 8, Apr. 2022, doi: 10.3390/SU14084539.

[7]   M. Wicht and K. Osinska-Skotak, "Identifying urban areas prone to flash floods using GIS &ndash; preliminary results," *Hydrology and Earth System Sciences Discussions*, no. October, pp. 1–22, 2016, doi: 10.5194/hess-2016-518.

[8]   F. Radwan, A. Alazba, and A. Mossad, "Watershed morphometric analysis of Wadi Baish Dam catchment area using integrated GIS-based approach," *undefined*, vol. 10, no. 12, Jun. 2017, doi: 10.1007/S12517-017-3046-5.

[9]   M. Attwa and A. Henaish, "Regional structural mapping using a combined geological and geophysical approach – A preliminary study at Cairo-Suez district, Egypt," *Journal of African Earth Sciences*, vol. 144, pp. 104–121, Aug. 2018, doi: 10.1016/J.JAFREARSCI.2018.04.010.

[10]   R. Said, "Review of the Geology of Egypt: by Rushdi Said," *American Journal of Science*, vol. 262. pp. 1237–1238, 1964.

[11]   P. Panagos, A. Jones, C. Bosco, and P. S. Senthil Kumar, "European digital archive on soil maps (EuDASM): Preserving important soil data for public free access," *Int J Digit Earth*, vol. 4, no. 5, pp. 434–443, 2011, doi: 10.1080/17538947.2011.596580.

[12]   S. Moustafa, A. R., El-Nahhas, F., & Abdel Tawab, "Structural Setting of the Area East of Cairo, Maadi, and Helwan.," *Middle East Research Center, Ain Shams University Scientific Research Series.*, vol. 5, pp. 40–64, 1985.

[13]   M. G. Shukri, N.M, AKMAL, "The geology of gebel EL Nasuri and Gebel EL Anqabiya district," 1953.

[14]   H. A. Wanas, M. M. Khalifa, and F. A. Mousa, "A contribution to the lithostratigraphy of the Plio-Pleistocene succession in the area southwest of Wadi El-Natrun , north Western Desert , Egypt A contribution to the lithostratigraphy of the Plio-Pleistocene succession in the area southwest of Wadi El-N," no. January, pp. 0–28, 2020.

[15]   M. el Bastawesy, M. Attwa, T. H. Abdel Hafeez, and A. Gad, "Flash floods and groundwater evaluation for the non-gauged dryland catchment using remote sensing, GIS and DC resistivity data: A case study from the Eastern Desert of Egypt," *Journal of African Earth Sciences*, vol. 152, pp. 245–255, Apr. 2019, doi: 10.1016/J.JAFREARSCI.2019.02.004.

[16]   O. Anomohanran and M. E. Orhiunu, "Assessment of groundwater occurrence in Olomoro, Nigeria using borehole logging and electrical resistivity methods," *Arabian Journal of Geosciences*, vol. 11, no. 9, May 2018, doi: 10.1007/S12517-018-3582-7.